TISSUE ENGINEERING: Part A
Volume 28, Numbers 19 and 20, 2022

DOI: 10.1089/ten.tea.2021.0217

termis
Tissue Engineering
& Regenerative Medicine
International Society

Open camera or QR reader and scan code to access this article and other resources online.

ORIGINAL ARTICLE

Donor Age and Time in Culture Affect Dermal Fibroblast Contraction in an *In Vitro* Hydrogel Model

Amber Detwiler, BS,[1–3] Kathryn Polkoff, PhD,[1,3] Lewis Gaffney, PhD,[1,2]
Donald O. Freytes, PhD,[1,2] and Jorge A. Piedrahita, PhD[1,3]

Current cellular hydrogel-based skin grafts composed of human dermal fibroblasts and a hydrogel scaffold tend to minimize contraction of full-thickness skin wounds and support skin regeneration. However, there has been no comparison between the sources of the dermal fibroblast used. Products using human adult or neonatal foreskin dermal fibroblasts are often expanded *in vitro* and used after multiple passages without a clear understanding of the effects of this initial production step on the quality and reproducibility of the cellular behavior. Based on the known effects of 2D tissue culture expansion on cellular proliferation and gene expression, we hypothesized that differences in donor age and time in culture may influence cellular properties and contractile behavior in a fibroblast-populated collagen matrix. Using porcine skin as a model based on its similarity to human skin in structure and wound healing properties, we isolated porcine dermal fibroblasts of three different donor ages for use in a 2D proliferation assay and in a 3D cell-populated collagen matrix contractility assay. In 2D cell culture, doubling time remained relatively consistent between all age groups from passage 1 to 6. In the contractility assays, fetal and neonatal groups contracted faster and generated more contractile force than the adult group at passage 1 *in vitro*. However, after five passages in culture, there was no difference in contractility between ages. These results show how cellular responses in a hydrogel scaffold differ based on donor age and time in culture *in vitro*, and suggest that consistency in the cellular component of bioengineered skin products could be beneficial in the biomanufacturing of consistent, reliable skin grafts and graft *in vivo* models. Future research and therapies using bioengineered skin grafts should consider how results may vary based on donor age and time in culture before seeding.

Keywords: cell proliferation, collagen, dermis, extracellular matrix, fibroblasts, hydrogels, skin, wound healing

Impact Statement

Little is known about the impact of donor cell age and time in culture on the contraction of cellular, hydrogel-based skin grafts. These results show how cellular phenotypes of porcine fibroblasts differ based on donor age and time in culture. This information is beneficial when addressing important inconsistencies in biomanufacturing of bioengineered skin grafts and *in vitro* models. These findings are relevant to research and therapies using bioengineered skin graft models and the results can be used to increase reproducibility and consistency during the production of bioengineered skin constructs. The information from this study can be extrapolated to future *in vivo* studies using human dermal fibroblasts in an *in vivo* model to help determine the best donor age and time in culture for optimal wound healing outcomes or more reproducible *in vitro* testing constructs.

[1]Comparative Medicine Institute, North Carolina State University, Raleigh, North Carolina, USA.
[2]Joint Department of Biomedical Engineering, North Carolina State University/University of North Carolina-Chapel Hill, Raleigh, North Carolina, USA.
[3]Department of Molecular Biomedical Sciences, North Carolina State University, Raleigh, North Carolina, USA.

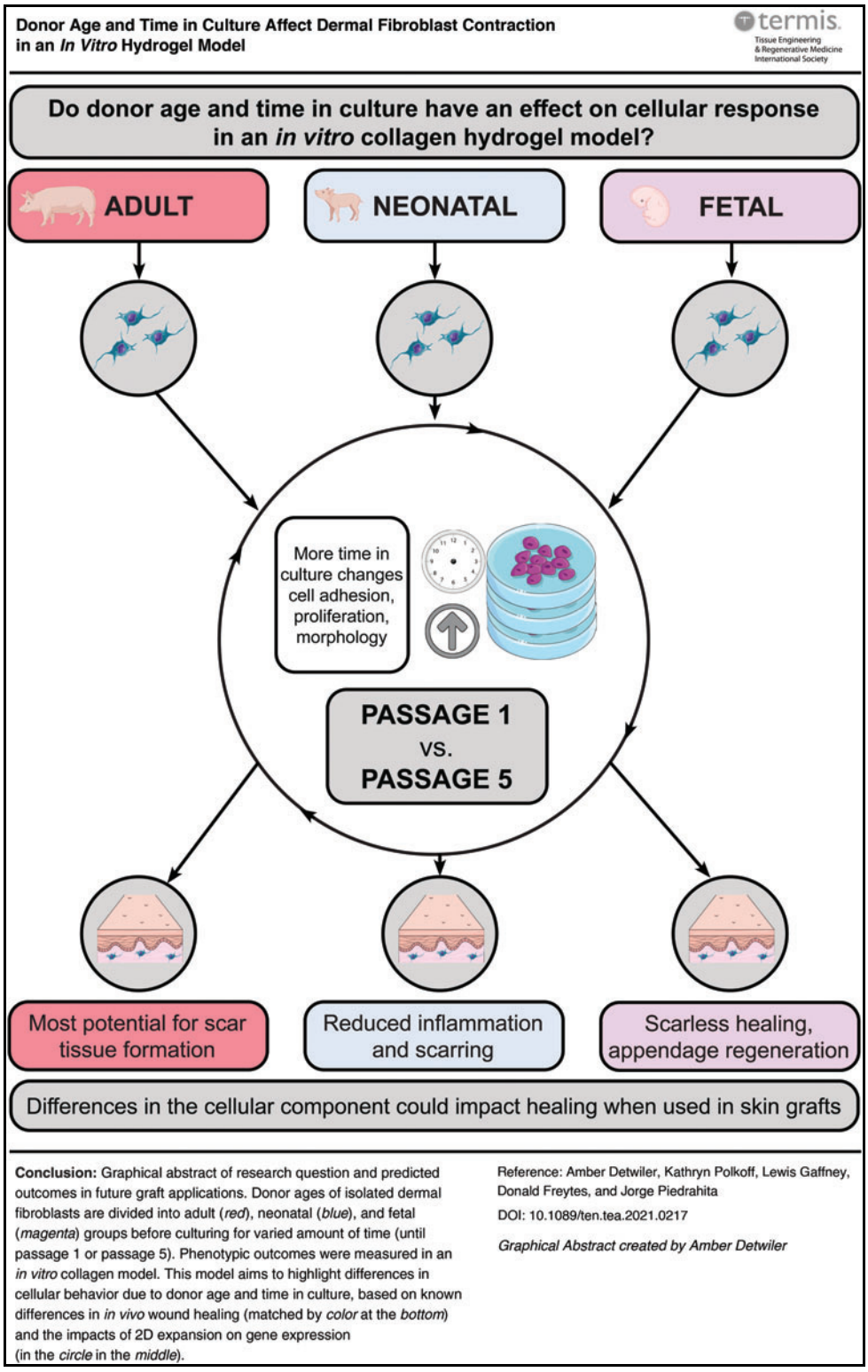

(Color images are available online)

Introduction

DUE TO THE vital functional role skin plays in protection, insulation, and prevention of water loss, severe skin injuries such as burns and deep wounds can be debilitating and life-threatening.[1,2] Skin grafting is performed annually in 30% of burn hospitalizations and as treatment for chronic skin wounds.[3,4] While autologous skin transplants for full-thickness skin wounds is common, it is not a viable treatment for larger, more severe wounds due to insufficient donor material to cover the affected area. Engineered biomaterials can substitute autologous grafts, thus eliminating

the need for harvesting autologous tissues, while also supporting more natural healing. Many bioengineered grafts utilize a hydrogel-cell construct, which focuses on mimicking the dermis by isolating and seeding dermal fibroblasts in a collagen-based hydrogel. These hydrogels can be created as a singular layer or bilayer dermal graft.

While there are many acellular skin grafts on the market, they do not address the poor barrier function of grafts without a cellular component, while also promoting extracellular matrix (ECM) deposition, secreting growth factors, and lengthening the time that the graft covers the wound.[5] The cellular component of skin grafts may consist of patient-derived dermal fibroblasts that are isolated and expanded for use or from other sources such as neonatal foreskin dermal fibroblasts, given their availability and perceived notion that they will be more resilient and promote faster healing due to their neonatal phenotype. A summary of current skin grafts and skin models currently on the market, including human dermal fibroblast cell age and time in culture at seeding, is shown in Table 1.

Even with differences in donor age (neonate to adult with no definition of adult age) and time in culture (passage 1–8) at seeding among grafts and skin models (Table 1), little is known about whether variability in the cellular component causes different properties in the graft, thus affecting its manufacturability and eventual utility for wound healing applications. We studied this cellular component using porcine dermal fibroblasts as a model, hypothesizing that dermal fibroblasts of differing donor age and time in culture behave differently in a hydrogel scaffold.

This hypothesis was based on differences in levels of regeneration, scarring, and contraction observed *in vivo* during healing between fetal, neonatal, and adult skin, as well as the impact of increased 2D culture on cellular morphology and phenotype. *In vivo* wound healing studies show differences between adult and neonatal skin, with neonates exhibiting faster re-epithelization, reduced inflammation and scarring, and better regeneration of natural tissue structure.[19] *In vivo* studies have also shown that fetal skin can undergo scarless healing, contrary to comparably wounded adult skin, which cannot heal to its original state and instead forms scar tissue lacking skin appendages.[20] Two-dimensional culture does not accurately mimic conditions *in vivo* and increased time in culture in this environment has been found to disturb cell-matrix interactions and even alter cell morphology, division method, and cell polarity.[21]

Because of all these properties, we hypothesized that donor age and increased time in culture of the dermal fibroblast component affect cellular response when seeded in a collagen hydrogel, which could have further impacts on consistency in biomanufacturing of skin grafts and models. A porcine model was chosen based on research by Sullivan *et al.*, which found that porcine wound healing models agree with human studies 78% of the time, whereas small-animal studies agree only 53% of the time.[22] Porcine skin is similar to human skin in thickness, hair distribution, and coat attachment.[22] Hamilton *et al.* suggest that the pig is the most similar model for wound healing in humans, particularly in terms of myofibroblast behavior.[23] Pigs are also frequently used for preclinical testing of autologous cellular therapies, as described by Thangapazham *et al.* who noted the use of porcine dermal fibroblasts in a porcine wound model.[24]

To examine the phenotypic behavior of dermal fibroblasts, changes in contractile and growth properties of a collagen-based hydrogel containing fibroblasts of varying donor age and time in culture were measured. Understanding the impact of these factors on cellular behavior is important for their application in skin grafts and models, and could be beneficial in improving wound healing outcomes and increasing reproducibility across skin grafts and models with additional research.

Table 1. Examples of Hydrogel-Based Skin Grafts and Skin Models on the Market

	Manufacturer	*Cell type*	*Cell age*	*Time in culture at seeding*	*Singular layer/ bilayer*	*Biomaterial*	*Source(s)*
Graft							
Transcyte	Advanced Tissue Sciences	Allogenic	Neonatal	Passage 8	Singular layer	Nylon mesh with a silastic layer	6
Apligraf	Organogenesis, Inc.	Allogenic	Neonatal	Passage 5–7	Bilayer	Bovine collagen type I	7
Dermagraft	Organogenesis, Inc.	Allogenic	Neonatal	Passage 8	Singular layer	Polyglycolic acid mesh	8
MyDerm	Universiti Kebangsaan Malaysia	Autologous	Adult	Passage 3	Bilayer	Plasma fibrin	9,10
OrCel	Forticell Bioscience, Inc.	Allogeneic	Neonatal	Passage 4	Bilayer	Type I bovine collagen sponge	11,12
PermaDerm	Regenicin	Autologous	Adult	Passage 2	Bilayer	Absorbable collagen substrate	13
StrataGraft	Stratatech Corp.	Allogenic	Adult or Neonatal	Not specified	Bilayer	Murine collagen	14,15
Model							
Phenion	Henkel	Allogenic	Neonatal	Passage 1	Bilayer	Not specified	16,17
EpiDerm-FT	MatTek Corp.	Allogenic	Adult or Neonatal	Not specified	Bilayer	Not specified	18

Human dermal fibroblast cell type (allogenic or autologous), cell age (adult and/or neonatal), and time in culture at seeding (passage number) are shown for comparison.

Materials and Methods

Primary cell isolation

Porcine dermal fibroblasts were isolated from fetal (isolated on day 42 of pregnancy), neonatal (<24 h after birth), and adult (over 6 months) dermis in this study. This study was carried out in strict accordance with the recommendations in the Guide for the Care and Use of Laboratory Animals of the National Institutes of Health[25] and approved by the Institutional Animal Care and Use Committee of North Carolina State University.

Dermis was removed from gestational day 42 fetal pigs and the tissue was then digested in a 0.025% trypsin and 0.5% ethylenediaminetetraacetic acid solution in a 37°C tumbling incubator for 45 min. An equal volume of alpha Dulbecco's modified Eagle medium (DMEM) was added to resuspend the cell suspension in medium. Cells were cultured at 37°C for at least 3–5 days, checking for attachment and adding media if necessary, and then split after 6–10 days. At 80% confluence, the fetal fibroblasts were harvested and frozen in dermal freezing media (6:3:1 ratio of DMEM, fetal bovine serum [FBS], and dimethyl sulfoxide, respectively).

Adult and neonatal dermal fibroblasts were isolated by first removing fat and shaving hair from a fresh porcine skin sample and dicing prepared skin into 2–3 mm square pieces and incubated at 4°C overnight in a 10 mg dispase per milliliter of 1 × Dulbecco's phosphate-buffered saline (PBS) solution. After manually separating the dermis from the epidermis, the dermis was digested in 4 mg collagenase per 1 mL DMEM in a rolling incubator at 37°C for 1–3 h. After vortexing the dermis in solution in three, 10-s intervals, the liquid was filtered with a 100 μm filter and frozen in dermal freezing media, and stored at −80°C before transfer to liquid nitrogen until use.

Proliferation assay

For the proliferation assay, cells were seeded at a known cell density of 2.2×10^5 in a six-well plate. Fibroblasts were passaged with 0.05% trypsin when confluent and counted with an automatic cell counter. Doubling time was then calculated using the following formula:

$$N_t = N_0 2^{tf} \quad (1)$$

where N_t is the number of cells at passage, N_0 is the number of cells seeded initially, t is the time in hours from seeding to passage, and $\frac{1}{f}$ is the doubling time in hours. Doubling times were calculated using cells that had undergone at least one passage after thawing (apart from passage 1). This assay was performed with at least two biological replicates and three technical replicates at each age and passage.

Actin cytoskeleton assay

Cells were cultured in six-well plates in DMEM with 15% FBS and 1% antibiotic/antimycotic until they reached 30–50% confluency. Fixation was performed by first rinsing with PBS and then fixing directly within the six-well plate using 1 mL of 4% paraformaldehyde per well for 15 min at room temperature. Wells were rinsed thrice with PBS before permeabilizing with 1 mL per well of 0.5% Triton X-100 in PBS for 15 min at room temperature. After rinsing each well three times with PBS, the samples were blocked with 3% bovine serum albumin in PBS for at least 1 h.

ActinGreen (phalloidin) and 4′,6-diamidino-2-phenylindole (DAPI) ReadyProbes (Invitrogen) were added to the block as per manufacturer's instructions and incubated at room temperature for 30 min before imaging. Imaging was performed on a Leica fluorescent microscope at 20 × magnification, with two representative photos taken of each well. This assay was performed with three biological replicates and three technical replicates at each age and passage.

Image analysis was performed using ImageJ. Individual fluorescent channels were thresholded to identify the DAPI-stained areas in the blue channel and actin-stained regions in the green channel. The thresholded area of actin was measured in pixels and the number of cell nuclei was counted using the Analyze Particles plugin, manually adding any overlapping nuclei. Finally, the actin area was divided by the number of nuclei in each image to get a measure of actin (area of positive pixels) per cell.

Hydrogel creation

For every 1 mL of a hydrogel of ECM concentration 6 mg/mL, the following were combined on ice: 600 μL Bovine Type-1 Collagen (Advanced BioMatrix), 275 μL 1 × PBS, 67 μL 10 × PBS, and 5 μL phenol red as a pH indicator. This mixture was vortexed to combine before adding 90 μL of 0.1 M sodium hydroxide and vortexing again, changing the color from the yellow, acidic pH, to a pink, neutral pH. To seed the hydrogel with cells, the gel was diluted to an ECM concentration of 3 mg/mL by adding an equal volume of cell suspension in DMEM. This process is simplified in Figure 2A. The gels used in this study were seeded at a density of 1.5×10^6 cells/mL. This mixture was vortexed to combine and plated accordingly.

Contraction assay

For the contraction assay, the hydrogel/cell mix described above was plated 0.5 mL per well in a 24-well plate, avoiding bubbles. The hydrogels were incubated at 37°C for 15–30 min, or until set, before gently detaching the gel from the well sides with a pipette tip and adding 1 mL DMEM with 15% FBS and 1% antibiotic/antimycotic. The contraction assay was repeated with fibroblasts isolated from at least two different pigs of the same age and cultured to the same passage (either passage 1 or 5) before seeding. The assay for each sample had at least two technical replicates. One well was seeded without any cells and only collagen hydrogel to act as a control, with no contraction expected in this well.

Photos were taken every day for 5–7 days after seeding. Percent contraction as determined by surface area was calculated in ImageJ and MATLAB was used to calculate the day at which each sample reached a threshold of 70% of total contraction.

Micropost assay

A micropost assay was used to measure force generation of the cells in the hydrogel, as done by Nandi *et al.*[26]

Microposts were created using polydimethylsiloxane in a 3D printed mold. These microposts were then plasma treated and stored in deionized water. Right before use, the microposts were sterilized with 70% ethanol and set out to air dry under a hood. The microposts were then coated with 0.3% bovine serum albumin for 10 min, aspirated to dry, and seeded with hydrogel. Approximately 1.5 μL of hydrogel of the same cell density and ECM concentration of the contraction assay was pipetted into each micropost.

The gels were incubated for 15–30 min, or until set, before gently adding 1 mL DMEM with 15% FBS and 1% antibiotic/antimycotic to the microposts in the well of a 24-well plate. Since the same hydrogel/cell mix was used in the micropost assay as was used in the contraction assay, the hydrogel-only well described in the contraction assay protocol also acted as a control for the micropost assay. The micropost assay was performed with at least two biological replicates and at least two technical replicates.

Photos were taken every day for 5–7 days after seeding. Force generation was calculated with the equation $F = k\delta$, where F is the force in micronewtons (μN) applied to cause the micropost deflection, k is the spring constant of the microposts, and δ is the deflection distance (μm). ImageJ was used to measure deflection, and the constant k was assumed to equal 7.5 newtons per meter.[26]

Gene expression analysis

RNA extraction was performed using a Zymo RNeasy Mini-Prep Kit. Dermal fibroblasts were suspended in lysis buffer immediately after passages 1 and 5 according to the manufacturer's instructions with the on-column DNAse digest. cDNA was synthesized according to the Agilent AffinityScript cDNA Synthesis Kit protocol. Polymerase chain reaction (PCR) products were run using gel electrophoresis to confirm that product sizes matched those shown in Supplementary Table S1.[27–34] For gene expression analysis, each of the genes in Supplementary Table S1 was measured by real-time PCR (RT-qPCR) in the qTOWER3 by Analytik Jena with the iTaq Universal SYBR Green Supermix kit with GAPDH (glyceraldehyde 3-phophate dehydrogenase) as the control. ddCt values were then normalized to passage 1 for each age group (i.e., adult passage 5 was normalized to adult passage 1, neonatal passage 5 to neonatal passage 1, etc.). Three biological replicates were analyzed for each age and passage number.

Statistical analysis

Micropost assay, contraction assay, and actin cytoskeleton data were analyzed using an unpaired, two-tailed *t*-test. Pearson correlation coefficient was calculated for the actin cytoskeleton assay, and the resulting test statistic was used to measure statistical significance. The qPCR data were analyzed using Welch's *t*-test for comparison between passage 1 and passage 5 data within each age group in GraphPad Prism. Significance was set at $p < 0.05$.

Results

Measured proliferation was consistent across cell ages

Dermal fibroblasts isolated as shown in Figure 1A were frozen immediately after isolation at passage zero before being thawed and plated for use in the proliferation assay. No morphological difference in fibroblasts based on age was noted (Fig. 1B–D). All age groups decreased in doubling time with a smaller standard deviation immediately after passage 1 and into passage 2 (Fig. 1E). No other notable difference in doubling time was noted between age groups and passages, indicating consistent proliferation from passages 1 to 6 as measured by doubling time.

Adult fibroblasts contract collagen gel less than other ages at passage 1

To determine the differences in contractile properties across age groups after minimal culture, we first measured the impact of donor age upon the rate of contraction of collagen hydrogels. After seeding the dermal fibroblasts within a collagen hydrogel as shown in Figure 2A, the change in area was measured over the course of 5 days. The adult dermal fibroblasts (Fig. 2C) took significantly longer time than the other two groups to reach the contractile threshold of 70% of total contraction (Fig. 2D, E).

To quantitatively confirm the effectiveness of the contraction assay in accurately measuring contractile forces, force generation was measured using a micropost assay (Supplementary Fig. S1A). Neonatal and fetal dermal fibroblasts generated more force than adult fibroblasts, although only fetal and adult were found to be statistically significantly different (Supplementary Fig. S1B). Based on the similar contractile force generation results of the contraction assay and micropost assay at passage 1, the contraction assay alone was deemed sufficient to measure contractile forces for samples seeded at passage 5.

Contraction was similar between age groups and faster within groups at passage 5

Since many of the products on the market expand the fibroblasts in culture (Table 1) before using, the next step was to determine how serial passaging of the fibroblasts would impact hydrogel contraction. Passage 5 was chosen as the average of passages provided in Table 1. Results from contraction of passage 5 cells overlaid with passage 1 cells show that the neonatal and fetal donors have similar contraction curves at both passages, but the adult dermal fibroblasts contracted faster at passage 5 than passage 1 (Fig. 2C).

Comparison of contraction rate (time required for gel to contract to 70% of total contraction) showed that fetal contracted faster than adult ($p = 0.001$) and neonatal faster than adult ($p = 0.02$) (Fig. 2F). When seeded at passage 5, however, there was no statistically significant difference between any age group. This is because, while the neonatal group contraction did not change between P1 and P5 ($p = 0.57$), the adult and fetal groups demonstrated significantly increased contraction after 5 passages ($p = 0.004$ and 0.04, respectively). These results suggest that, although there were significant differences in contraction of early passage cells based on donor age, after five passages, their behavior was more homogenous and suggests that time in culture generally increases contractile properties of fibroblasts.

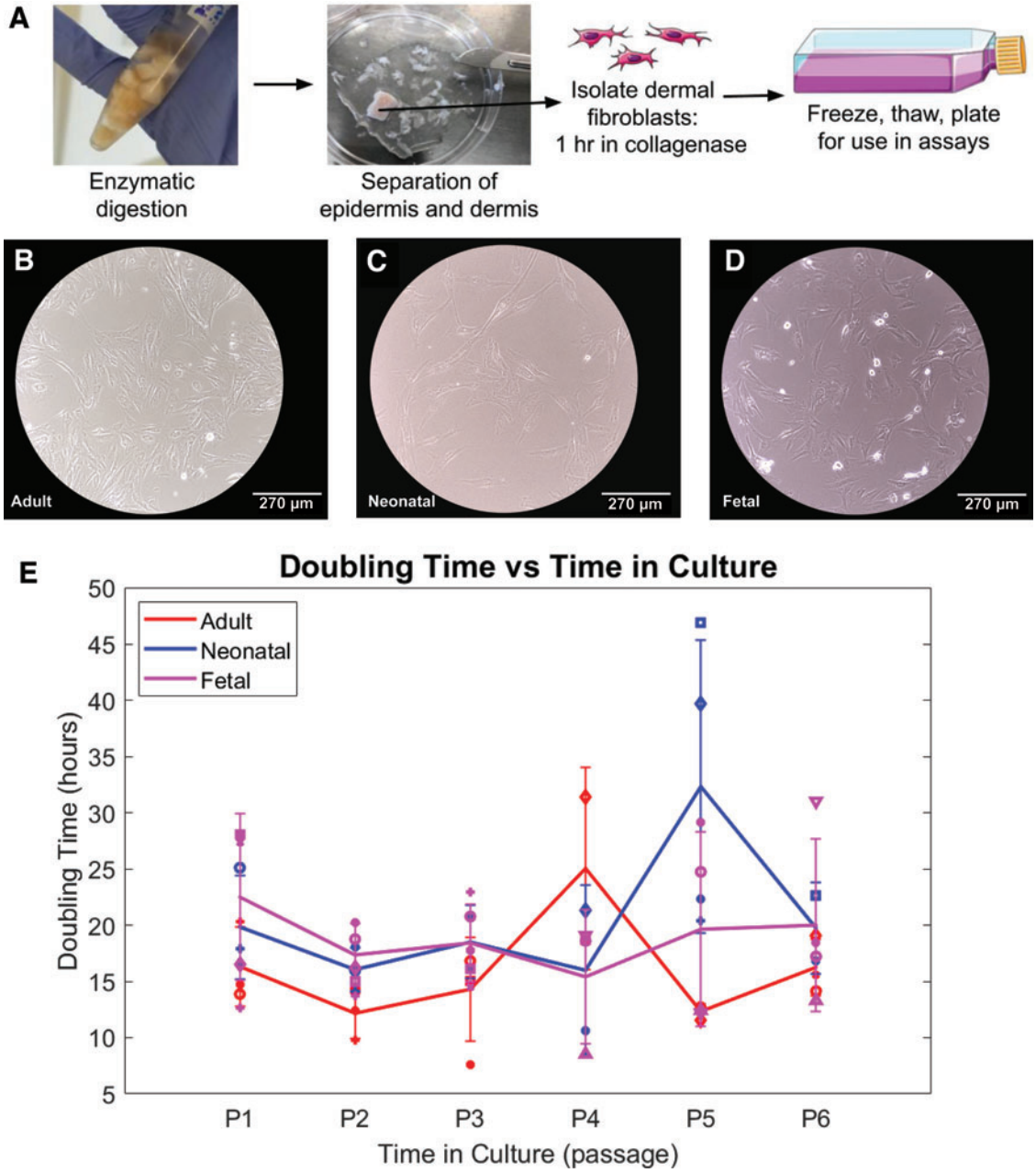

FIG. 1. Proliferation measured by doubling time remained relatively consistent between adult, neonatal, and fetal fibroblasts at passages 1–6. **(A)** Schematic illustration of primary cell isolation of dermal fibroblasts and epidermis from porcine skin. **(B–D)** Brightfield 10×image of passage 1 adult, neonatal, and fetal dermal fibroblasts in 2D culture. **(E)** Average doubling time in hours for adult (*red*), neonatal (*blue*), and fetal (*magenta*) samples from passage 1 to passage 6. Each marker *shape* corresponds to a different sample for that age group. Cells from at least two different pigs were analyzed at each passage, with three technical replicates of each cell sample averaged to produce each point above. Color images are available online.

Actin cytoskeleton was significantly larger for neonatal fibroblasts at passage 5 versus 1

Based on the association between upregulation of actin and increased fibroblast contractile activity, a fluorescent stain for F-actin was used to compare the cytoskeleton of fibroblasts of different donor age and passage.[35] Differences in cytoskeleton based on donor age and time in culture were quantified by calculating the area of cytoskeleton per cell. As shown in Figure 3G, neonatal dermal fibroblasts exhibited a significantly larger cytoskeleton area per cell at passage 5 compared to passage 1 ($p=0.01$), as well as between fetal at passage 5 ($p=0.02$) and adult at passage 5 ($p=0.02$). To compare to the contraction results in Figure 2, actin expression was plotted versus days to contract to the 70% threshold, as shown in Figure 2F. There was a nonsignificant correlation ($p=0.27$) between actin expression and contraction with a Pearson correlation coefficient of $r=-0.514$ (Fig. 3H).

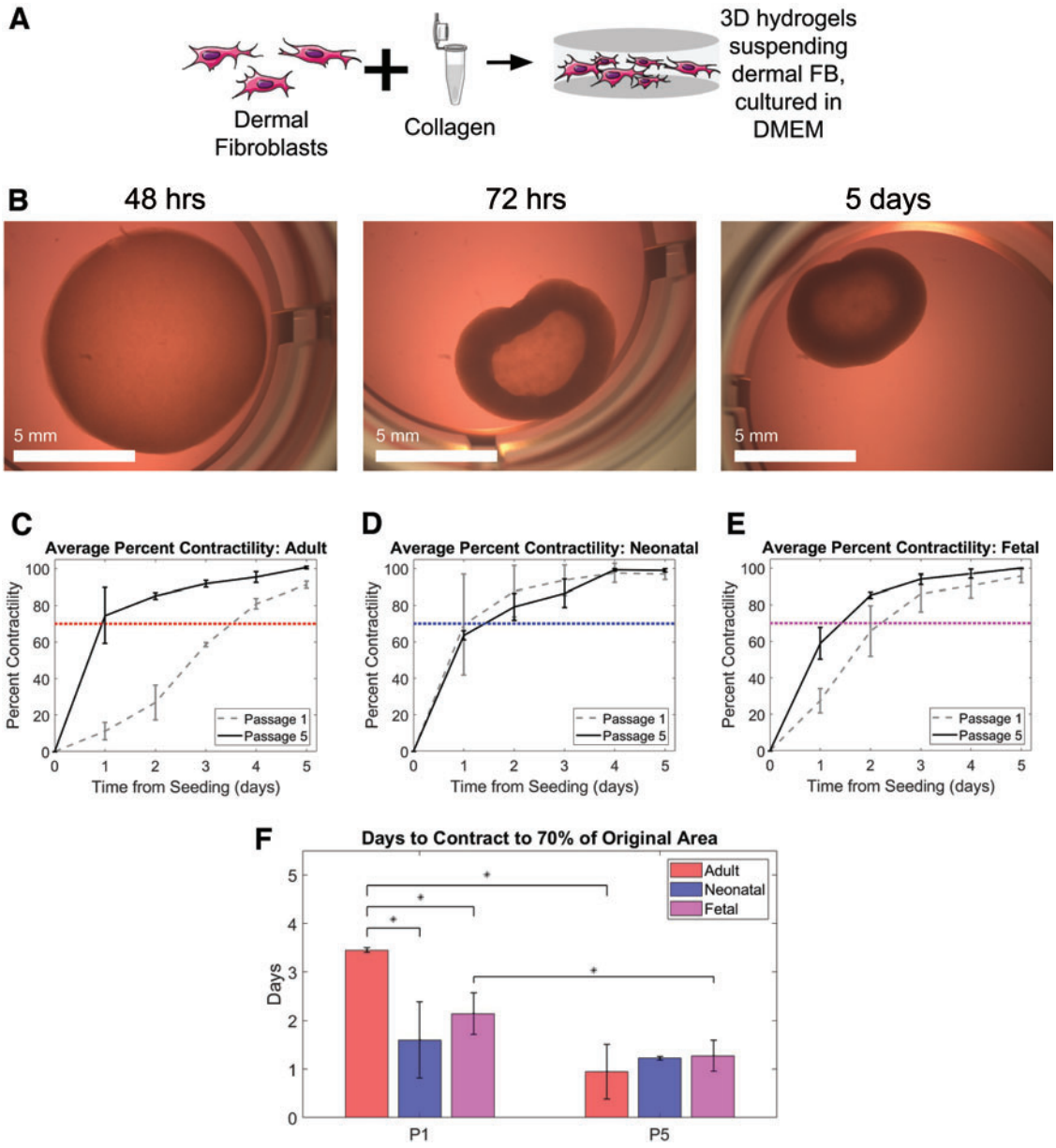

FIG. 2. Adult dermal fibroblasts contracted slower than neonatal and fetal when seeded at P1. Adult, neonatal, and fetal age groups experienced similar contraction between age groups, and faster contraction within age groups when seeded at P5. **(A)** Schematic illustration displaying the combining of dermal fibroblasts and bovine type I collagen gel to culture in 3D. **(B)** Fetal fibroblasts seeded in collagen contractility assay at 48 h, 72 h, and 5 days after seeding. **(C–E)** Average percent contractility from day 0 (seeding) to day 5 was found based on the percent difference in surface area, which was then normalized to maximum contraction for easier comparison. Adult (*left*, *red*), neonatal (*middle*, *blue*), and fetal (*right*, *magenta*) shown. Data for cells seeded at passage 1 are shown in *dashed gray* and those seeded at passage 5 are shown in *black*. A threshold of 70% is shown in *dotted red*, *blue*, and *magenta* for adult, neonatal, and fetal, respectively. **(F)** Time in days for each age group to contract to a threshold of 70%, grouped by the passage number of cells at seeding (passage 1 on *left* and passage 5 on *right*). Passage 5 was chosen as the approximate average of the existing human bioengineered skin equivalents listed in Table 1, and is compared to passage 1, which represents minimal time in culture before seeding. Statistical significance between groups with an alpha value of 0.05 is indicated by an * and bars indicate standard deviation. Cells from at least two different pigs with three technical replicates were analyzed in each group. Color images are available online.

Effect of passage on TAZ, STAT1, *and* COL1A2 *expression*

To further understand differences in the cellular phenotype that could contribute to the contraction observed in Figure 2, gene expression analysis was performed focusing on nine genes involved in wound healing, contraction, and ECM deposition.

From passage 1 to passage 5, *TAZ* fold change showed a statistically significant difference within adult, neonatal, and fetal groups with p-values of 0.002, 0.03, and 0.02, respectively (Fig. 4A). *STAT1* significantly increased from neonatal

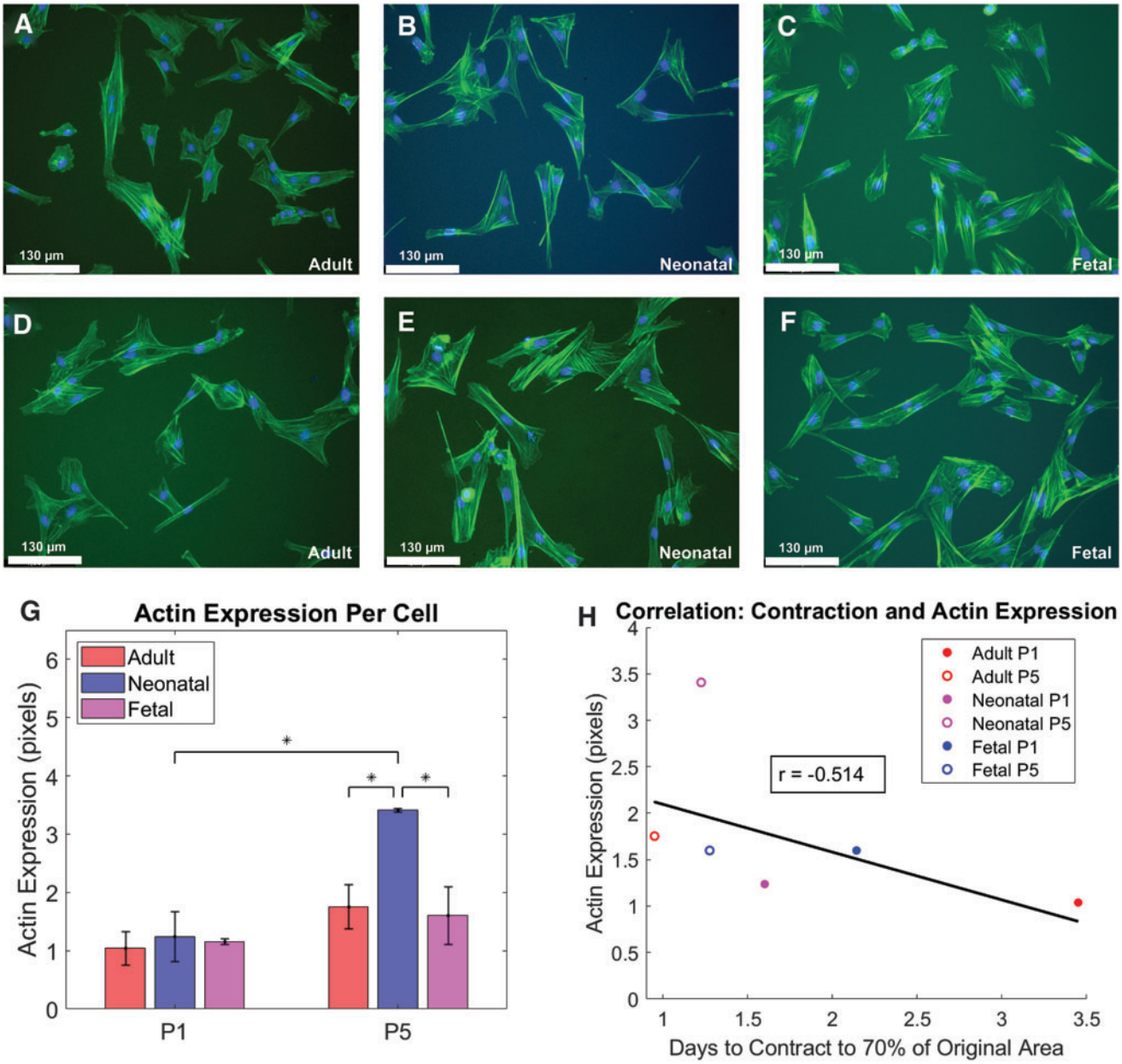

FIG. 3. Actin cytoskeleton was significantly larger for neonatal fibroblasts at passage 5 versus 1. **(A–C)** Fluorescent 20×images of passage 1 adult, neonatal, and fetal dermal fibroblasts in 2D culture. **(D–F)** Fluorescent 20×images of passage 5 adult, neonatal, and fetal dermal fibroblasts in 2D culture. All fluorescent images were stained with DAPI and actin. **(G)** Average actin expression in pixels per cell for each donor age and time in culture, grouped by the passage number of cells at seeding (passage 1 on *left* and passage 5 on *right*). Statistical significance between groups with an alpha value of 0.05 is indicated by an * and bars indicate standard deviation. **(H)** Plot of average actin expression per cell (pixels) versus days to reach the 70% contraction threshold. *Red*, *blue*, and *magenta circles* correspond to adult, neonatal, and fetal groups, respectively. Passage number is marked by *openness* of the *circle*, with the *filled circles* representing passage 1 and the *open circles* representing passage 5. Cells from at least two different pigs were analyzed at each passage and age, with three technical replicates of each cell sample averaged to produce each point above. DAPI, 4′,6-diamidino-2-phenylindole. Color images are available online.

passage 1 to neonatal passage 5 with a *p*-value of 0.03 (Fig. 4B). The adult group saw a significant increase from passage 1 to 5 for fold change in expression of *COL1A2* with a *p*-value of 0.02 (Fig. 4C). Genes which showed no statistically significant difference in expression are shown in Supplementary Figure S2.

Discussion

The focus of this research was to look more closely at the potential effects of culture conditions of the cellular component of bioengineered skin grafts using a porcine model. Specifically, the goal was to understand how donor age and

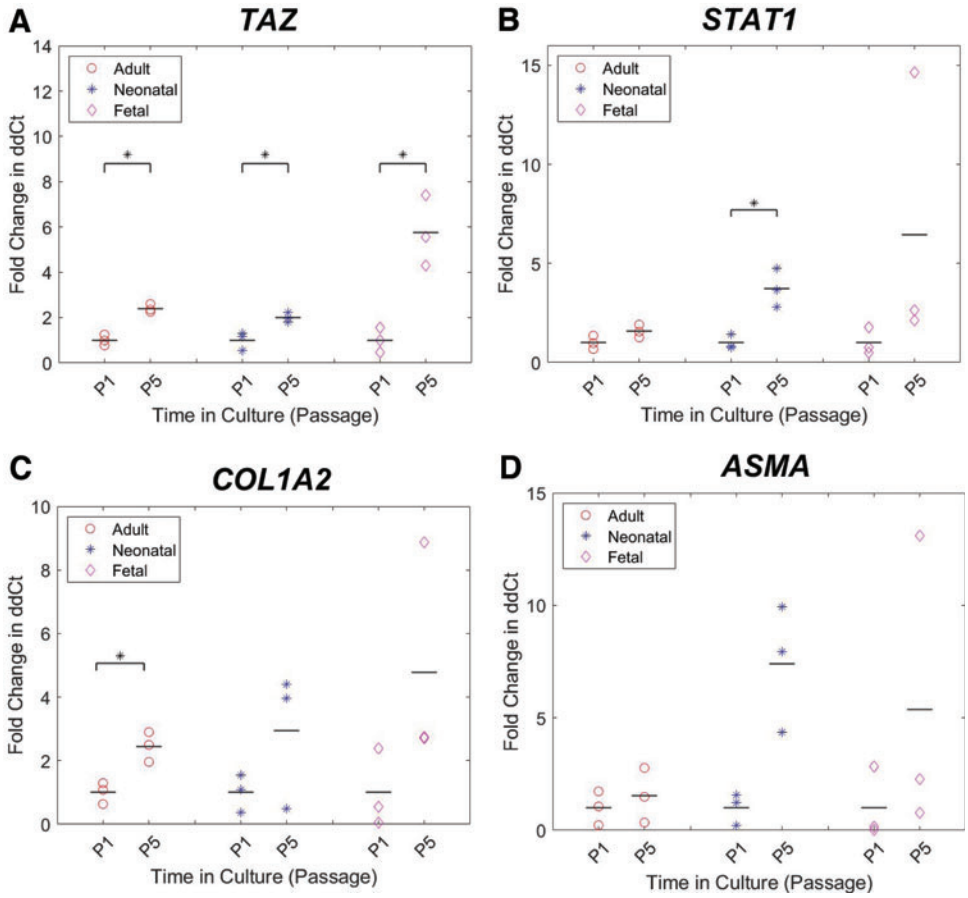

FIG. 4. Gene expression analysis for a panel of genes related to wound healing, contraction, and ECM deposition. **(A–D)** Fold change in ddCt from passage 1 to 5 for adult (*red circle*), neonatal (*blue cross*), and fetal (*magenta diamond*) dermal fibroblasts. These comparisons are based on passage 5 as the approximate average of the existing human bioengineered skin equivalents listed in Table 1, and passage 1 as the minimal time in culture before seeding. The mean for each group is indicated by a *black bar*. dCt values were standardized to GAPDH, followed by ddCt values where adult passage 5 was standardized to adult at passage 1, neonatal passage 5 to neonatal passage 1, and so on. Cells from at least two different pigs with three technical replicates were analyzed in each group. Statistical significance between groups with an alpha value of 0.05 is indicated by a *black bar* and *. ECM, extracellular matrix; GAPDH, glyceraldehyde 3-phophate dehydrogenase. Color images are available online.

time in culture affect fibroblast behavior and contraction of a fibroblast-populated collagen matrix. Given the inconsistencies in donor age and time in culture for skin grafts and models on the market, this research suggests that there may be differences in cellular behavior based on those found using this initial porcine dermal fibroblast and collagen hydrogel model. Understanding and addressing these differences could be beneficial in manufacturing a more consistent and predictable skin graft model.

Doubling time remained relatively consistent between all age groups across the first six passages, suggesting that increased expansion on tissue culture plastic did not have any major effect on fibroblast proliferation rates. Based on this fibroblast proliferation and growth rate, there appears to be no advantage to expanding one donor age or passage over another. However, gene expression analysis of donor cells found *TAZ*, *STAT1*, and *COL1A2* expression to significantly increase from passage 1 to passage 5 in some groups, suggesting that increased time in culture before seeding may affect graft/skin model behavior, given the potential phenotypic changes suggested by the measured gene expression. This phenotypic change should be explored in more detail in future studies.

Contraction was similar between age groups at passage 5, but not at passage 1. These results are supported by Hopp *et al.*, which found substrate stiffness to affect adhesion, proliferation, and morphology, meaning that increased time in culture on stiff tissue culture plastic causes the cells to behave differently when moved to the much less stiff hydrogel environment.[36] While the time to reach 70% contraction decreased significantly from passage 1 to passage 5 in the adult fibroblast-populated collagen matrix, there was no significant difference in the neonatal model from passage 1 to passage 5. This could suggest that neonatal donor cells present more a consistent phenotype and predictable contraction at a range of passages.

However, the actin cytoskeleton was found to significantly increase from passage 1 to passage 5 in neonates, suggesting that time in culture may still impact the

contractile behavior of neonatal fibroblasts. Alternatively, adult donor fibroblasts may allow for tunable contraction based on time in culture before seeding.

This research establishes—in an initial porcine model—that donor age and time in culture at seeding should be considered and standardized for reproducibility and consistency across human graft products. The similar contraction behavior among age groups at passage 5 as opposed to passage 1 offers more consistency in the cellular component of the graft, including more usable cells per donor tissue, and potentially more predictable scaffold needs. Overall, these results provide insight into fibroblast behavior in an *in vitro* collagen hydrogel based on age and time in culture, factors that may also apply to the cellular component of skin grafts and the outcomes of those grafts when applied *in vivo*.

Current skin grafts are known to reduce wound contraction and scarring compared to healing by secondary intention; however, contraction after initial skin graft application can create a need for surgical release and application of additional skin graft.[37] For skin wounds near joints, this can increase the risk for graft failure and total cost of treatment.[37] Similarly, *in vitro* skin model contraction can result in detachment of the epidermal layer from the insert wall, creating a less-functional skin model.[38] Research has focused on graft contraction based on matrix formation and properties, including the effects of temperature on plasma-based hydrogel contraction,[39] and reduced graft contraction with cross-linked collagen[38] and nanofibrillar cellulose[40] hydrogels.

While a fibroblast-populated collagen matrix is by no means a full measure of the complete nuances of *in vivo* wound healing contraction, the different contractile properties based on donor age and time in culture could foreshadow different graft outcomes based on the characteristics of cells seeded in the graft. Cellular phenotype as measured by proliferation, protein synthesis, contraction, and cell viability has been shown to be similar between *in vivo* wound healing models and the *in vitro* fibroblast-populated collagen matrix model.[41] The contraction of the fibroblast-populated collagen matrix is an indicator of cell activation, with this behavior associated with *in vivo* wound healing.[42] This research shows differing cellular phenotypes *in vitro* based on donor age and time in culture, and could suggest different *in vivo* wound healing outcomes due to these varying cellular phenotypes.

Future assays expanding on these results should assess gene expression in human dermal fibroblasts at a broader range of cell donor ages and time in culture and compare the cell types discussed *in vivo*. This research is useful for all current and future applications of cellular hydrogel-based skin grafts and could also aid in determining which donor age is best for supporting skin appendage regeneration in biomaterial skin grafts.

Conclusions

Findings show that in 2D cell culture, doubling time remained relatively consistent between all age groups from passage 1 to 6. Contraction of collagen hydrogels differed significantly based on donor age as well as time in culture at seeding. Gene expression analysis of donor cells showed changes in *TAZ*, *STAT1*, and *COL1A3* with increased time in culture. These results provide support for differing cellular phenotypes *in vitro* as a function of age and time in culture, which may also foreshadow differences in the cellular component of skin grafts and models for use *in vivo*.

Acknowledgments

The authors thank the Comparative Medicine Institute, the NC State University and University of North Carolina at Chapel Hill Joint Department of Biomedical Engineering, and the NC State College of Veterinary Medicine for making this research experience possible. The authors would like to acknowledge that this article was previously submitted as a preprint on BioRxiv.org (doi: 10.1101/2021.11.29.469875).

Authors' Contributions

A.H.D. wrote the article, and planned and executed the studies presented. K.M.P. and L.S.G. wrote the article, planned experiments, and assisted with execution of studies presented. D.O.F and J.A.P. assisted in writing the article, planned experiments, and oversaw execution of studies presented.

Disclosure Statement

No competing financial interests exist.

Funding Information

Funding for this research was provided by the Comparative Medicine Institute, the NC State University Office of Undergraduate Research, and the Department of Biomedical Engineering Abrams Scholar Program. Additional support comes from NIH F31AR077423 to Kathryn Polkoff.

Supplementary Material

Supplementary Table S1
Supplementary Figure S1
Supplementary Figure S2

References

1. Nadel ER, Bullard RW, Stolwijk JA. Importance of skin temperature in the regulation of sweating. J Appl Physiol 1971;31(1):80–87; doi: 10.1152/jappl.1971.31.1.80.
2. Dąbrowska AK, Spano F, Derler S, *et al.* The relationship between skin function, barrier properties, and body-dependent factors. Skin Res Technol 2018;24(2):165–174; doi: 10.1111/srt.12424.
3. McDermott KW, Weiss AJ, Elixhauser A. Burn-Related Hospital Inpatient Stays and Emergency Department Visits, 2013: Statistical Brief# 217. Rockville, MD: Agency for Healthcare Research and Quality; 2017.
4. Valencia IC, Falabella AF, Eaglstein WH. Skin grafting. Dermatol Clin 2000;18(3):521–532; doi: 10.1016/s0733-8635(05)70199-6.
5. Chocarro-Wrona C, López-Ruiz E, Perán M, *et al.* Therapeutic strategies for skin regeneration based on biomedical

substitutes. J Eur Acad Dermatol Venereol 2019;33(3): 484–496; doi: 10.1111/jdv.15391.
6. Mansbridge J. Chapter 81—Tissue-engineered skin products. In: Principles of Tissue Engineering, 4th ed. (Lanza R, Langer R, Vacanti J, eds.) Academic Press: Boston; 2013; pp. 1697–1715.
7. Wilkins LM, Watson SR, Prosky SJ, *et al.* Development of a bilayered living skin construct for clinical applications. Biotechnol Bioeng 1994;43(8):747–756; doi: 10.1002/bit.260430809.
8. Naughton G, Mansbridge J, and Gentzkow G. A Metabolically active human dermal replacement for the treatment of diabetic foot ulcers. Artif Organs 1997;21(11):1203–1210; doi: 10.1111/j.1525–1594.1997.tb00476.x.
9. Seet WT, Manira M, Khairul Anuar K, *et al.* Shelf-life evaluation of bilayered human skin equivalent, MyDerm™. PLoS One 2012;7(9):e40978; doi: 10.1371/journal.pone.0040978.
10. Mohamed Haflah NH, Ng MH, Mohd Yunus MH, *et al.* Massive traumatic skin defect successfully treated with autologous, bilayered, tissue-engineered MyDerm skin substitute: A case report. JBJS Case Connect 2018;8(2): e38; doi: 10.2106/JBJS.CC.17.00250.
11. Eisenberg M, Llewelyn D. Surgical management of hands in children with recessive dystrophic epidermolysis bullosa: Use of allogeneic composite cultured skin grafts. Br J Plast Surg 1998;51(8):608–613; doi:10.1054/BJPS.1998.9997.
12. Halim AS, Khoo TL, Mohd Yussof SJ. Biologic and synthetic skin substitutes: An overview. Indian J Plast Surg 2010;43(Suppl):S23–S28; doi: 10.4103/0970-0358.70712.
13. Boyce ST, Kagan RJ, Greenhalgh DG, *et al.* Cultured skin substitutes reduce requirements for harvesting of skin autograft for closure of excised, full-thickness burns. J Trauma 2006;60(4):821–829; doi: 10.1097/01.ta.0000196802.91829.cc.
14. Nathoo R, Howe N, Cohen G. Skin substitutes: An overview of the key players in wound management. J Clin Aesthet Dermatol 2014;7(10):44–48.
15. Pipeline | Mallinckrodt Pharmaceuticals [Internet]. Mallinckrodt. [Cited June 14, 2020]. Available from: www2.mallinckrodt.com/research/science-technology/pipeline/ (accessed June 14, 2020).
16. Henkel. Reconstructed Tissues [Internet]. [Cited April 11, 2021]. Available from: https://www.phenion.com/products/reconstructed-tissues (accessed April 11, 2021).
17. Yun YE, Jung YJ, Choi YJ, *et al.* Artificial skin models for animal-free testing. Int J Pharm Investig 2018;48(2):215–223; doi:10.1007/s40005-018-0389-1.
18. Kubilus J, Hayden P, Burnham B, *et al.* Full thickness EpiDerm™: A dermal–epidermal skin model to study epithelial–mesenchymal interactions. Altern Lab Anim 2004;32(1 Suppl):75–82; doi: 10.1177/026119290403201s12.
19. Wagner W, Wehrmann M. Differential cytokine activity and morphology during wound healing in the neonatal and adult rat skin. J Cell Mol Med 2007;11(6):1342–1351; doi: 10.1111/j.1582–4934.2007.00037.x.
20. Lo DD, Zimmermann AS, Nauta A, *et al.* Scarless fetal skin wound healing update. Birth Defects Res C Embryo Today 2012;96(3):237–247; doi: 10.1002/bdrc.21018.
21. Kapałczyńska M, Kolenda T, Przybyła W, *et al.* 2D and 3D cell cultures—A comparison of different types of cancer cell cultures. Arch Med Sci 2018;14(4):910–919; doi: 10.5114/aoms.2016.63743.
22. Sullivan TP, Eaglstein WH, Davis SC, *et al.* The pig as a model for human wound healing. Wound Repair Regen 2001;9(2):66–76; doi: 10.1046/j.1524-475x.2001.00066.x.
23. Hamilton DW, Walker JT, Tinney D, *et al.* The pig as a model system for investigating the recruitment and contribution of myofibroblasts in skin healing. Wound Repair Regen 2022;30(1):45–63; doi: 10.1111/wrr.12981.
24. Thangapazham RL, Darling TN, Meyerle J. Alteration of skin properties with autologous dermal fibroblasts. Int J Mol Sci 2014;15(5):8407–8427; doi: 10.3390/ijms15058407.
25. National Research Council, Division on Earth and Life Studies, Institute for Laboratory Animal Research, and Committee for the Update of the Guide for the Care and Use of Laboratory Animals. Guide for the Care and Use of Laboratory Animals: Eighth Edition. Washington, DC: National Academies Press; 2011
26. Nandi S, Sproul EP, Nellenbach K, *et al.* Platelet-like particles dynamically stiffen fibrin matrices and improve wound healing outcomes. Biomater Sci 2019;7(2):669–682; doi: 10.1039/c8bm01201f.
27. Opiela J, Lipiński D, Romanek J, *et al.* MMP-2, TIMP-2, TAZ and MEF2a transcript expression in osteogenic and adipogenic differentiation of porcine mesenchymal stem cells. Ann Anim Sci 2016;16(2):369–385; doi: 10.1515/aoas-2015-0065.
28. Dawson HD, Royaee AR, Nishi S, *et al.* Identification of key immune mediators regulating T helper 1 responses in swine. Vet Immunol Immunopathol 2004;100(1–2):105–111; doi: 10.1016/j.vetimm.2004.03.006.
29. Cai L, Sun A, Li H, *et al.* Molecular mechanisms of enhancing porcine granulosa cell proliferation and function by treatment in vitro with anti-inhibin alpha subunit antibody. Reprod Biol Endocrinol 2015;13(1):1–10; doi: 10.1186/s12958-015-0022-3.
30. Sriperumbudur R, Zorrilla L, Gadsby JE. Transforming growth factor-beta (TGFbeta) and its signaling components in peri-ovulatory pig follicles. Anim Reprod Sci 2010;120(1–4):84–94; doi: 10.1016/j.anireprosci.2010.03.003.
31. Sood RF, Muffley LA, Seaton ME, *et al.* Dermal fibroblasts from the red duroc pig have an inherently fibrogenic phenotype: An in vitro model of fibroproliferative scarring. Plast Reconstr Surg 2015;136(5):990–1000; doi: 10.1097/PRS.0000000000001704.
32. Yang J, Li K, Liu B, *et al.* Assignments of GRB7, GCN5L2, COL1A1 and TBCD to pig chromosome 12 by radiation hybrid mapping. Cytogenet Genome Res 2003;103(1–2):204L; doi: 10.1159/000076312.
33. Warnecke C, Kaup D, Marienfeld U, *et al.* Adenovirus-mediated overexpression and stimulation of the human angiotensin II type 2 receptor in porcine cardiac fibroblasts does not modulate proliferation, collagen I mRNA expression and ERK1/ERK2 activity, but inhibits protein tyrosine phosphatases. J Mol Med 2001;79(9):510–521; doi: 10.1007/s001090100243.
34. Bao X, Zeng Y, Wei S, *et al.* Developmental changes of Col3a1 mRNA expression in muscle and their association

with intramuscular collagen in pigs. J Genet Genomics 2007;34(3):223–228; doi: 10.1016/S1673–S8527(07) 60023-X.
35. Hinz B, Celetta G, Tomasek JJ, *et al.* Alpha-smooth muscle actin expression upregulates fibroblast contractile activity. Mol Biol Cell 2001;12(9):2730–2741; doi: 10.1091/mbc.12.9.2730.
36. Hopp I, Michelmore A, Smith LE, *et al.* The influence of substrate stiffness gradients on primary human dermal fibroblasts. Biomaterials 2013;34(21):5070–5077; doi: 10.1016/j.biomaterials.2013.03.075.
37. Harrison CA, MacNeil S. The mechanism of skin graft contraction: An update on current research and potential future therapies. Burns 2008;34(2):153–163; doi: 10.1016/j.burns.2007.08.011.
38. Lotz C, Schmid FF, Oechsle E, *et al.* Cross-linked collagen hydrogel matrix resisting contraction to facilitate full-thickness skin equivalents. ACS Appl Mater Interfaces 2017;9(24):20417–20425; doi: 10.1021/acsami.7b04017.
39. Montero A, Acosta S, Hernández R, *et al.* Contraction of fibrin-derived matrices and its implications for in vitro human skin bioengineering. J Biomed Mater Res A 2021;109(4):500–514; doi: 10.1002/jbm.a.37033.
40. Nuutila K, Laukkanen A, Lindford A, *et al.* Inhibition of skin wound contraction by nanofibrillar cellulose hydrogel. Plast Reconstr Surg 2018;141(3):357e–366e; doi: 10.1097/PRS.0000000000004168.
41. Carlson MA, Longaker MT. The fibroblast-populated collagen matrix as a model of wound healing: a review of the evidence. Wound Repair Regen 2004;12(2):134–147; doi: 10.1111/j.1067–1927.2004.012208.x.
42. Smithmyer ME, Sawicki LA, Kloxin AM. Hydrogel scaffolds as in vitro models to study fibroblast activation in wound healing and disease. Biomater Sci 2014;2(5):634–650; doi: 10.1039/C3BM60319A.

Address correspondence to:
Donald O. Freytes, PhD
Joint Department of Biomedical Engineering
North Carolina State University
University of North Carolina-Chapel Hill
4208D Engineering Building III
Campus Box 7115
Raleigh, NC 27695
USA

E-mail: dofreyte@ncsu.edu; dfreytes@unc.edu

Jorge A. Piedrahita, PhD
Comparative Medicine Institute
North Carolina State University
Biomedical Partnership Center 20001
Campus Box 8401
Raleigh, NC 27695
USA

E-mail: japiedra@ncsu.edu

Received: February 2, 2022
Accepted: May 31, 2022
Online Publication Date: August 5, 2022